Bisurea-Functionalized RAFT Agent: A Straightforward and Versatile Tool toward the Preparation of Supramolecular Cylindrical Nanostructures in Water

Gaëlle Mellot, Jean-Michel Guigner, Jacques Jestin, Laurent Bouteiller, Francois Stoffelbach, Jutta Rieger

Bisurea-functionalized RAFT agent: a straightforward and versatile tool towards the preparation of supramolecular cylindrical nanostructures in water

Gaëlle Mellot,[†] Jean-Michel Guigner,[‡] Jacques Jestin,[$] Laurent Bouteiller,[†] François Stoffelbach[†] and Jutta Rieger[*†]*

[†]Sorbonne Université, CNRS, Institut Parisien de Chimie Moléculaire, UMR 8232, Equipe Chimie des Polymères, F-75252 Paris Cedex 05 (France).

[‡]Sorbonne Université, CNRS, Institut de Minéralogie, de Physique des Matériaux et de Cosmochimie, UMR 7590 - IRD - MNHN, F-75005 Paris (France).

[$]Laboratoire Léon Brillouin, UMR12 CEA-CNRS, Bât. 563, CEA Saclay, 91191 Gif-sur-Yvette Cedex, France

TABLE OF CONTENTS

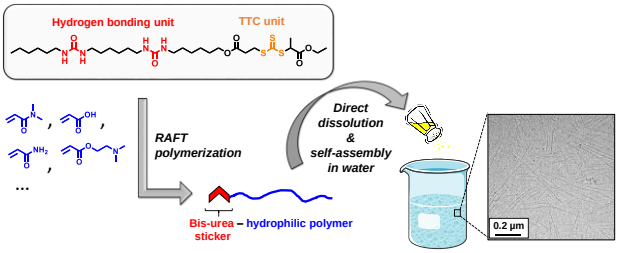

(for Table of Contents use only)

KEYWORDS

RAFT polymerization, H-bonding, cylindrical micelles, ITC

ABSTRACT

We report a versatile and simple approach to produce cylindrical micelles by the direct dissolution of polymers in water. The developed strategy relies on a RAFT agent functionalized by a bisurea sticker that allowed to synthesize a series of α-bisurea functionalized poly(*N,N*-dimethylacrylamide) (PDMAc), poly(acrylic acid) (PAA), polyacrylamide (PAM) and poly(2-(*N,N*-dimethylamino)ethyl acrylate) (PDMAEA) with number-average degrees of polymerization (DP_n) varying from about 10 to 50. Their spontaneous self-assembly in water was studied by electron microscopy (cryo-TEM), neutron scattering (SANS) and calorimetry (ITC) analyses that showed that long cylindrical micelles are spontaneously formed in water. The crucial role of the bisurea sticker end-groups was established by comparison with the corresponding bisurea-free model polymers that only formed spherical micelles. Finally, we have shown that it is possible to trigger reversibly the assembly/disassembly of the nanofibers by pH changes.

Introduction

One-dimensional nano-assemblies driven by supramolecular interactions are ubiquitous in Nature and show a rich variety of functions. In the past decade, the preparation of cylindrical objects by spontaneous self-assembly of synthetic building blocks in water has therefore been a major objective. Such assemblies have indeed a huge potential for various applications in material science, ranging from biomedical applications[1] to reinforcement of water-based acrylic coatings[2], and their use as templates for catalysis[3] or as stabilizer of Pickering emulsions.[4] Inspired by natural systems, directional supramolecular interactions have been used to drive the

assembly of synthetic macromolecules[5] in water into cylindrical nanostructures. In that respect, the introduction of π-π interacting aromatic functional units and/or hydrogen-bonding (H-bonding) units within water-soluble macromolecules has become an efficient strategy.[5,6] In the latter case, it is well-known that water competes with H-bonding, and that a hydrophobic environment is consequently needed to protect the interactions and to achieve robust supramolecular structures in water.[6]

One efficient chemistry to assemble water-soluble polymers into cylindrical structures - *via* directional H-bonding - are bisurea stickers.[7–11] For instance, Sijbesma and co-workers reported the formation of well-defined rod-like micelles in water through the spontaneous self-assembly of poly(ethylene glycol) (PEG) bolamphiphiles possessing an aliphatic bisurea sticker in their center.[7–9] Shortly after, Boué and co-workers designed aromatic bisurea functionalized PEG which self-assemble in a wide range of solvents into long rigid cylinders, which are in dynamic equilibrium with their unimers.[10] Beyond these examples, numerous other supramolecular motifs, such as ureido-pyrimidinone,[12] peptides,[13–15] cyclodextrins[16] or benzenetricarboxamide[17,18] have been used to direct the assembly of synthetic water-soluble macromolecules into cylindrical structures. In most of the studies, low molar mass polymers were used, in particular oligo(ethylene glycol)s, and their functionalization by the sticker units was achieved by post-polymerization strategies.[19–22] Considering the time-consuming processes necessary to prepare these polymers and purify them from unmodified counterparts, more straightforward and versatile synthetic strategies are highly desirable.

Reversible-deactivation radical polymerization (RDRP),[23] formerly called controlled radical polymerization, enables the synthesis of a wide range of well-defined polymeric architectures.[24,25] The reversible addition-fragmentation chain transfer (RAFT)[26] polymerization is nowadays recognized to be the most popular and versatile polymerization technique for the synthesis of complex and functional polymers. In particular, the reversible

chain transfer agent, called RAFT agent, can be functionalized by supramolecularly interacting units, such as H-bonding moieties,[27–32] π-π stacking moieties,[33] metal-ligand coordinating sites[34,35] or proteins[36] to synthesize functionalized polymers without demanding post-functionalization and separation processes to remove non-functional polymer. To the best of our knowledge, there is only one example that combines polymer functionalization through RAFT polymerization and directional supramolecular interactions in order to control the assembly of water-soluble polymers in water into cylindrical structures. In this recent study, Ghosh and coworkers designed a RAFT agent functionalized by a trialkoxybenzamide-linked naphthalene diimide (NDI) supramolecular structure directing unit (SSDU) which was used to synthesize a series of NDI-functionalized hydrophilic polymers (in part obtained through post-polymerization modifications). Freshly prepared aqueous polymer solutions contained mainly spherical micelles, which reorganized with time into cylindrical micelles.[37,38] Even if not formed spontaneously, the results clearly demonstrate that the cylindrical micelles were obtained thanks to directional stacking interactions of the NDI units overruling the packing parameter law.[39–41]

In the present work, we propose a new RAFT-polymerization based versatile synthesis strategy to access cylindrical nanostructures through spontaneous polymer dissolution in water. For this purpose, based on a known chemistry[8,42] we designed a simple bisurea-functionalized RAFT agent to be used as a platform to synthesize water-soluble polymers end-functionalized by a single SSDU, that drives their assembly in water through H-bonding interactions into cylindrical structures. To prove this concept and its versatility, we prepared a series of bisurea-end-functionalized polymers by RAFT polymerization and studied their self-assembly into cylindrical micelles in water. Finally, we tested also the possibility to control the micellar assembly and disassembly, or even to induce reversibly an inter-cylinder aggregation.

Experimental Section

Materials. 2,2'-azobis(2-amidinopropane) dihydrochloride (V-50, ≥ 97%, Aldrich), 2,2'-azobis(*N,N*-dimethyleneisobutyramidine) dihydrochloride (VA-044, 98%, Aldrich), 2,2′-azobis(isobutyronitrile) (AIBN, ≥ 98%, Aldrich), 1-ethyl-3-(3-dimethylaminopropyl)carbodiimide hydrochloride (EDC.HCl, ≥ 98%, TCI), 4-(dimethylamino)pyridine (DMAP, > 99%, Fluka), hydrogen chloride (*ca.* 4 mol L^{-1} in dioxane, TCI Europe), hexylamine (≥ 99%, Aldrich), hexamethylenediisocyanate (≥ 98%, Aldrich), triethylamine (≥ 99%, Aldrich), 1,4-dioxane (≥ 99%, Acros Organics) *N,N*-dimethylformamide (DMF, VWR, Normapur), acrylic acid (AA, ≥ 99%, Aldrich), acrylamide (AM, ≥ 99%, Aldrich) and 1,3,5-trioxane (≥ 99%, Aldrich) were used as received. 6-(Boc-amino)-1-hexanol (≥ 98%, Aldrich) and 1-octadecanol (99%, Aldrich) were dried by three successive azeotropic distillations with dry toluene before use. *N,N*-Dimethylacrylamide (DMAc, > 99%, Aldrich), and 2-(*N,N*-dimethylamino)ethyl acrylate (DMAEA, ≥ 99%, Abcr) were distilled under vacuum prior to polymerization. All aqueous solutions were prepared with deionized water. All syntheses and polymerizations were conducted under an argon atmosphere. CH_2Cl_2 (DCM) and toluene were dried by a solvent purification system (MBraun).

Analytical Techniques. The purity of RAFT agents was determined by ^{1}H NMR and ^{13}C NMR. Spectra were recorded at 298 K, with a Bruker 300 or 400 MHz spectrometer in 5-mm diameter tubes. Monomer conversions were determined by ^{1}H NMR spectroscopy in $CDCl_3$ or DMSO d_6 by the relative integration of the internal reference (1,3,5-trioxane) peak at 5.1 ppm and the vinylic monomer proton peaks. The number-average molar mass (M_n), the weight-average molar mass (M_w) and the dispersity ($Đ = M_w/M_n$) were determined by size exclusion chromatography (SEC) in DMF (+ LiBr, 1 g L^{-1}) at 60 °C and at a flow rate of 0.8 mL min^{-1}, using two PSS GRAM 1000 Å columns (8 × 300 mm; separation limits: 1 to 1000 kg mol^{-1}) and one PSS GRAM 30 Å (8 × 300 mm; separation limits: 0.1 to 10 kg mol^{-1}) coupled to a differential refractive index (RI) detector and a UV detector. Polymers containing AA units

have been modified by methylation of the carboxylic acidic groups using trimethylsilyldiazomethane before SEC analysis.[43] Cryogenic transmission electron microscopy (cryo-TEM) was used to determine the particle morphologies. The samples were dissolved in water to 1 wt% ~24 h before analysis (unless indicated differently below the figure). According to protocols reported elsewhere[44–46] thin liquid films of particle dispersions were prepared at room temperature by depositing 4 µL of the diluted sample and successive blotting. They were flash frozen in liquid ethane and observed at -180 °C on a JEOL JEM-2100 LaB_6 microscope operating at 200 kV under low-dose conditions (10 electrons $Å^{-2}$ s^{-1}). Digital images were recorded on a Gatan Ultrascan 1000 CCD camera. Isothermal titration calorimetry (ITC) measurements were performed at 25 °C using an ITC_{200} microcalorimeter. Solutions of PDMAc-U_2 and PDMAc-C_{18} (see SI) were freshly prepared in water at 0.88 mM, at room temperature the day of the experiment. According to procedures previously described,[47] the sample cell (202.7 µL) was filled with distilled water. Then an aqueous solution of PDMAc-U_2 (0.88 mM) placed in a continuously stirred (750 rpm) syringe (39 µL) was injected by aliquots (2 µL) every 180 s until the syringe was empty. The subsequent heat flow resulting from each injection was simultaneously measured.

Small-angle neutron scattering (SANS) measurements were made at the LLB (Saclay, France) on the PA20 SANS instrument, at three sample to detector distances 1.5, 8 and 18.5 m and fixed wavelength equal to 6 Å to cover the 2.5 10^{-3} to 0.44 $Å^{-1}$ q-range, where the scattering vector q is defined as usual, assuming elastic scattering ($q = (4\pi/\lambda)\sin(\theta/2)$, where θ is the angle between incident and scattered beam). Data were corrected for the empty cell signal, the solute and solvent incoherent background. A light water standard was used to correct from the detector in homogeneities and to normalize the scattered intensities to cm^{-1} units. The data was fitted with the DANSE software SasView.[48] The simplest model that allowed to fit all data was the sum of the form factor of an infinitely long core-shell cylinder with a circular cross-section and a short core-shell cylinder with the same contrast and cross-section dimension. The scattering length

densities for D_2O (6.37 10^{-6} $Å^{-2}$) and for the core (0.70 10^{-6} $Å^{-2}$) were calculated from the atomic bound coherent scattering lengths. The scattering length densities for the shell were adjusted during the simultaneous fit of all the data. The common value that allowed to fit all the systems was 4.68 10^{-6} $Å^{-2}$.

Synthesis of the bisurea-functional and octadecyl-endcapped model polymers

Polymerizations of DMAc, AA, AM and DMAEA in DMF were initiated by AIBN at 70 °C, in the presence of RAFT agent **TTC-U$_2$** or **TTC-C$_{18}$** (see Scheme S1 and S2). In a typical experiment (**D3**, Table 1), **TTC-U$_2$** (0.115 g, 0.18 mmol) was placed in a 5 mL round bottomed flask. 1,3,5-Trioxane (0.0215 g, 0.23 mmol) was then added as an internal reference for the determination of the monomer consumption by ^{1}H NMR in $CDCl_3$. A solution of AIBN (9.7 mg) in 16.8 g of DMF was prepared. 2.51 g of this solution (8.64 µmol of AIBN) was then added in the flask containing the RAFT agent. Then distilled DMAc (0.78 mL, 7.57 mmol) was added. After deoxygenation by bubbling with argon for 30 min in an ice bath, the septum-sealed flask containing the reaction mixture was heated at 70 °C in a thermostated oil bath. The polymerization was quenched after 75 min by immersion of the flask in iced water. The polymers were recovered by precipitation in diethyl ether (Et_2O) (in chloroform for the PAM), dried under reduced pressure and characterized by ^{1}H NMR in DMSO d_6 and SEC in DMF (+ LiBr, 1 g L^{-1}).

Results & Discussion

Synthesis of the bisurea-functional RAFT agent (TTC-U_2) and the model RAFT agent (TTC-C_{18})

The bisurea functional trithiocarbonate (TTC) RAFT agent (**TTC-U_2**, Scheme 1) was synthesized in four steps according to the strategy displayed in Scheme S1, starting from a carboxylic acid functional RAFT agent[49,50] (**TTC-0**, Scheme S1). Briefly, the first two steps consist in the synthesis of an amino-functional RAFT agent **TTC-2** obtained by esterification of **TTC-0** with 6-(tert-butoxycarbonylamino)-1-hexanol followed by the deprotection of the Boc group.[51] In parallel, 1-hexyl-3-(6-isocyanato-hexyl)-urea (**U_1-NCO**) was synthesized by reaction of *n*-hexylamine with hexamethylene diisocyanate according to a previously established protocol.[52] The targeted **TTC-U_2** was finally obtained by reacting a small excess of the amino-functional RAFT agent **TTC-2** with **U_1-NCO**. In view of the preparation of model polymers, in which the functional bisurea group is replaced by a hydrophobic octadecyl chain, an octadecyl RAFT agent **TTC-C_{18}** (Scheme 1) was also synthesized by esterification of **TTC-0** with *n*-octadecanol in the presence of EDC.HCl (Scheme S2). As reported in the Supporting Information (SI), the analytical data for both RAFT agents were consistent with the proposed structures (Figure S4 and S5).

Scheme 1. (A) Structures of the RAFT agents TTC-U_2 and TTC-C_{18}. (B) Synthesis of bisurea-functional polymers through RAFT-mediated polymerization in DMF à 70 °C

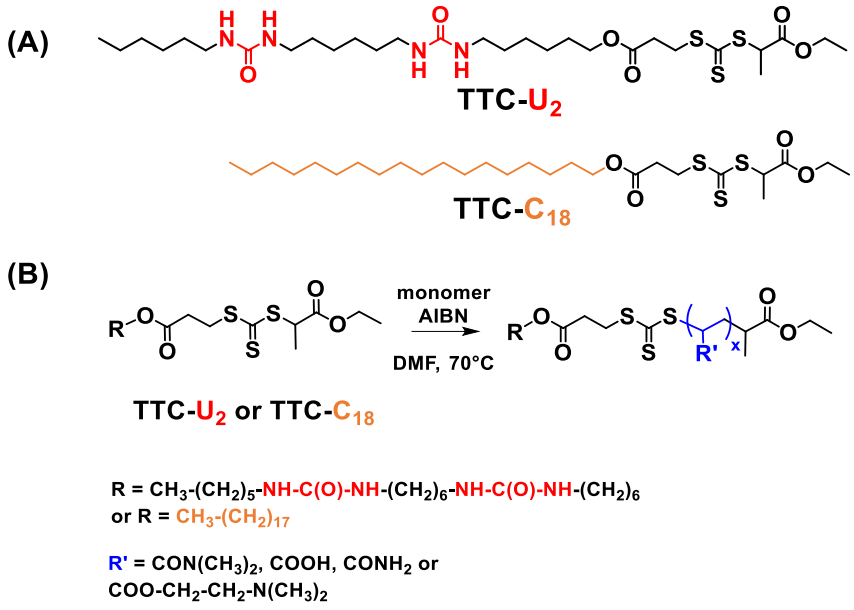

Synthesis of bisurea-functional polymers

The bisurea-functional RAFT agent **TTC-U$_2$** was used for the synthesis of bisurea-functional hydrophilic polymers (Scheme 1), namely poly(*N,N*-dimethylacrylamide) (PDMAc), poly(acrylic acid) (PAA), polyacrylamide (PAM), poly(2-(*N,N*-dimethylamino)ethyl acrylate) (PDMAEA). *N,N*-Dimethylformamide (DMF) – a good solvent for **TTC-U$_2$ -** was selected as a solvent for all polymerizations. According to previously established protocols,[53] all polymerizations were conducted at 70 °C using AIBN as an initiator. The polymerizations were generally quenched at conversions below 70% to limit the proportion of dead chains. For all polymer types a number-average degree of polymerization, DP_n, close to 20 was initially targeted (compare $DP_{n,conv.}$ **D2**, **AA2**, **AM2**, **DE3** in Table 1). In addition, a series of bisurea-functional PDMAc (PDMAc-U$_2$) was synthesized (D series: **D1**, **D2**, **D3** and **D4**) for which the targeted DP_n was systematically varied between approximately 10 and 40. The polymerization of DMAc progressed rapidly (70% monomer conversion was generally reached in 1 to 2h), but was slower in the case of AM, AA and DMAEA. ^{1}H-NMR analyses of the purified polymers in DMSO-d$_6$ showed well-defined signals characteristic of the bisurea functions (see for example spectrum of **D1** in Figure S6). The signals corresponding to the functional RAFT agent were compared to the integration of the protons of the polymer backbone to calculate the number-average molar mass (M_n) of the polymers (Table 1). Generally, the calculated M_n matched well the theoretical values indicating a high end-group functionalization. As summarized in Table 1, molar mass dispersities determined by size exclusion chromatography (SEC) analyses were below 1.2 for the PDMAc-U$_2$ series and PAA-U$_2$, and remained acceptable for PAM-U$_2$ and PDMAEA-U$_2$. Generally, during polymerizations molar masses increased linearly with monomer conversion (see for example data for **D4bis**, Figure S7), which is an additional sign for the control over polymerization. It should also be mentioned that the PDMAc series could successfully be reproduced demonstrating the robustness of the polymerization

conditions. The replica were named **D1bis**, **D2bis**, **D3bis** and **D4bis** (see data in the SI, Table S1 and Figure S8). For comparison, three bisurea-free PDMAc functionalized by a hydrophobic octadecyl alkyl chain were also synthesized using TTC-C_{18} (Scheme 1) as a RAFT agent. The results summarized in Table S2 show that the polymerizations were well controlled with dispersities close to 1.1 and the molar masses determined by ^{1}H-NMR were in good agreement with the theoretical values. Overall, no significant impact of the presence of the bisurea function on the polymerization control was observed. It can thus be concluded that the bisurea-functional RAFT agent TTC-U_2 allows the controlled synthesis of well-defined bisurea-functionalized polymers.

Table 1. Experimental conditions and results for the homopolymerizations of DMAc, AA, AM and DMAEA at 70 °C in DMF, in the presence of TTC-U_2 and AIBN as an initiator

Note: P*olymerizations are named X#, where X indicates the polymer and # the* $DP_{n,\,conv}$ *of the polymer divided by 10.*

Expt.	Monomer	$[Mono]_0$ / $[TTC]_0$	$[Mono]_0$ (M)	$[TTC]_0$/ $[AIBN]_0$	conv [a] (%) (time in min)	$DP_{n,conv}$ [a]	$M_{n,th}$ [b] (kg mol^{-1})	$DP_{n,NMR}$ [c]	$M_{n,NMR}$ [c] (kg mol^{-1})	$M_{n,SEC}$ [d] (kg mol^{-1})	$Đ$ [d]	*morpho cryo-TEM* [e]	d_n (C) [g] (nm)
D1	**DMAc**	14	2.0	20.3	69 (120)	10	1.6	11	1.7	1.7	1.18	C	6±1
D2	**DMAc**	29	2.0	19.9	67 (120)	19	2.6	20	2.6	2.3	1.13	C	8±1
D3	**DMAc**	43	2.2	20.4	68 (75)	29	3.6	35	4.1	3.2	1.17	S (C)	10±2
D4	**DMAc**	57	2.0	20.2	63 (375)	36	4.2	46	5.2	4.3	1.19	S (C)	13±4
AA2	**AA**	22	2.0	13.2	68 (270)	15	1.7	20	2.1	2.4[f]	1.15	C	5±1
AM1	**AM**	14	1.0	10.0	61 (200)	9	1.3	9	1.3	1.3	1.15	C	6±1
AM2	**AM**	28	2.0	10.1	76 (175)	22	2.2	24	2.4	0.7	1.39	S	/
DE3	**DMAEA**	50	3.2	5.5	57 (390)	29	4.8	32	5.2	3.7	1.66	C (S)	8±2

[a] Monomer conversion determined by ^{1}H NMR, used to calculate the theoretical $DP_{n,conv}$; [b] Theoretical number-average molar mass M_n at the experimentally determined conversion; [c] Number-average degree of polymerization, DP_n and number-average molar mass, M_n determined by ^{1}H NMR; [d] Number-average molar mass, M_n and dispersity, $Đ$, determined by size exclusion chromatography in DMF (+ LiBr, 1g L^{-1}) using poly(methyl methacrylate) standards; [e] Morphology observed by cryo-TEM after spontaneous dissolution in water at 1 wt% (without pH adjustment) S: spherical micelles, C: cylindrical micelles, the minority morphology is indicated in brackets; [f] M_n of the methylated polymer (cf. experimental section); [g] d_n (C) = number-average diameter of the cylinders determined by 40 measurements on cryo-TEM images.

Self-assembly of bisurea-functional poly(*N*,*N*-dimethylacrylamide) (PDMAc-U$_2$)

The aim of the study was the spontaneous formation of cylindrical polymer assemblies in water driven by directional supramolecular interaction of H-bonds present in the bisurea moiety at the end of the polymer chains. The water-solubility of the PDMAc-U$_2$ was therefore tested simply by adding water to the polymer powder. Whatever the molar mass, the polymers readily dissolved in water, at least in the tested range of concentration, up to 6 wt%. ^{1}H NMR of **D1bis** (Table S1) in D_2O showed the characteristic signals of the polymer, however the characteristics signals of the bisurea sticker, in particular the methyl end group were not detected (Figure S9), indicating the assembly of the polymer by interactions of the sticker. Then, the assembly of the polymers was studied by cryo-TEM on 1 wt% aqueous polymer solution. The cryo-TEM images of PDMAc-U$_2$ **D1** and **D2** with the lowest M_n undoubtedly showed the formation of cylindrical micelles (Figure 1A and 1B). These objects were observed after simple dissolution of the powder, without any heat or ultrasound treatment and no particular time evolution was noticed (between 75 minutes (Figure S10, **D1bis**, Table S1) and 24h (Figure 1A, **D1**, Table 1)). This shows that the self-assembly of PDMAc-U$_2$ is a spontaneous and fast process. This feature indicating a possibly dynamic assembly was later confirmed by ITC dilution experiments (cf. infra). By analogy with other amphiphiles that contain bisurea units,[7,8,10,54] we expect directional H-bonding between bisurea moieties to be responsible for the observed one-dimensional assembly into cylindrical nanoobjects. Actually, the same bisurea-motif had been previously incorporated in the center of short oligo(ethylene glycol) chains (M_n = 350 g mol^{-1}). Strongly aggregated rod-like micelles were formed that could be dispersed by ultrasound treatment.[7] In this former study, the corresponding bisurea-free amphiphilic counterpart however assembled into cylindrical micelles as well (albeit longer and well-separated).[7] We therefore also analyzed aqueous solutions of the bisurea-free octadecyl-capped model polymers (**M1** and **M2**, Table S2) by cryo-TEM. In this case, only spherical objects could be detected

(Figure 1E, 1F) confirming that in our study the bisurea is clearly responsible for the observed assembly into long cylindrical micelles.

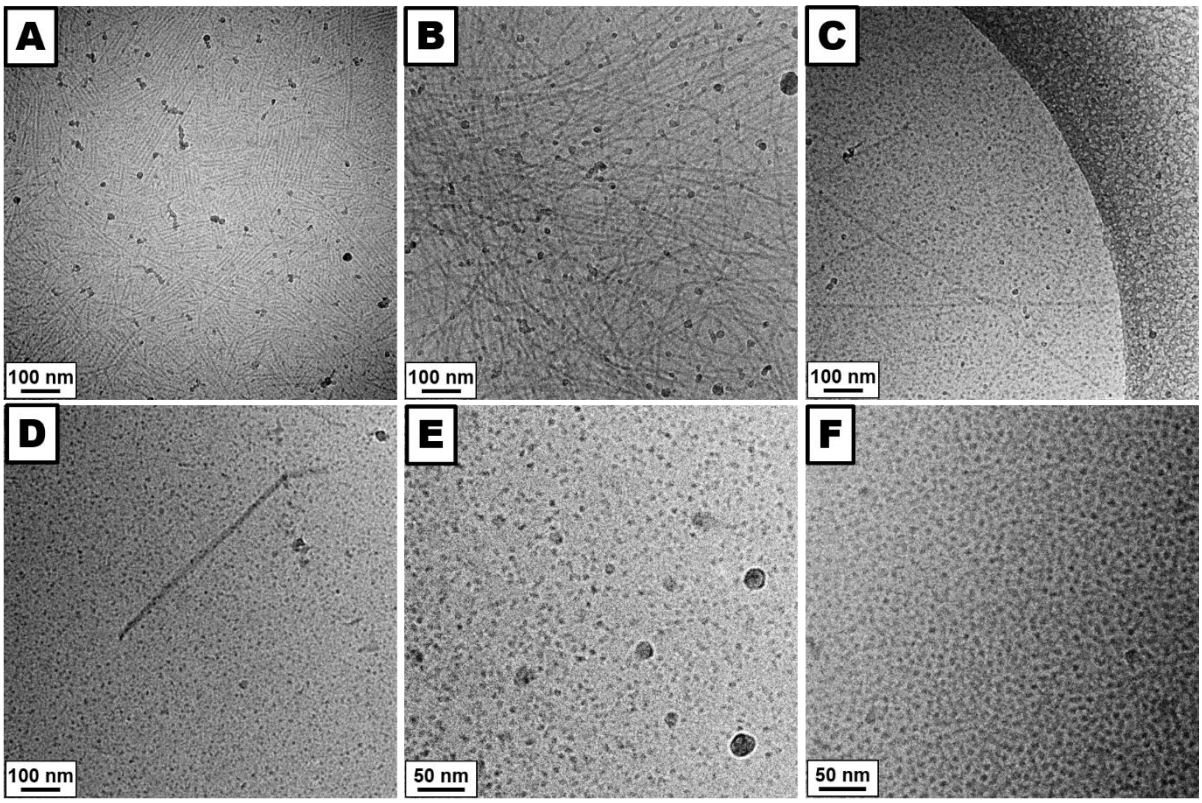

Figure 1. Representative cryo-TEM images of bisurea- and octadecyl-functional PDMAc assemblies (prepared at 1 wt% in water): (A) $PDMAc_{11}$-U_2 (**D1**), (B) $PDMAc_{20}$-U_2 (**D2**), (C) $PDMAc_{35}$-U_2 (**D3**), (D) $PDMAc_{46}$-U_2 (**D4**), (E) $PDMAc_{10}$-C_{18} (**M1**), and (F) $PDMAc_{19}$-C_{18} (**M2**). The dark spots are contaminations stemming from water crystals on the sample surface.

When the DP_n of PDMAc-U_2 was increased to 35 or 46, cylindrical micelles were still observed (polymers **D3** and **D4,** Figure 1C and 1D), but spherical micelles were also present and for the longest PDMAc only few cylindrical micelles – seemingly larger in diameter and shorter in length – were observed (see d_n (C) in Table 1). Thus, beyond a certain degree of polymerization, the directional supramolecular interactions seem to be overruled by steric effects of the PDMAc shell limiting the formation of cylindrical morphologies.[55]

To get more insights in the structure of the assemblies, small-angle neutron scattering (SANS) experiments were performed in deuterated water (D_2O) at 1 wt%, *i.e.* at the same concentration as the cryo-TEM analyses. Figure 2 shows the scattering patterns (intensity I (cm^{-1}) versus scattering vector q) obtained for the series of PDMAc-U_2 solutions after subtraction of the solvent scattering contribution. In the case of **D1** a q^{-1} dependence of the scattered intensity is clearly observed, which is characteristic for long and rigid objects. After normalization by the concentration, the data at 0.5 and 1 wt% were identical (Figure S11 shows the concentration-dependent scattering pattern for all PDMAc-U_2). This shows that interactions between scatterers can be neglected in this concentration range. Therefore, a fit of the data was attempted with the form factor of a core-shell cylinder with a circular cross-section.[48] A good fit was obtained for a core radius of 2.6 nm and a shell thickness of 1.7 nm (Table 2, see Experimental Section for more details). These values correspond reasonably well to the dimensions of the hydrophobic and solvated hydrophilic parts, respectively. The length of the cylinders could not be determined with precision due to the limited q-range available, but they can be considered to be at least 100 nm.

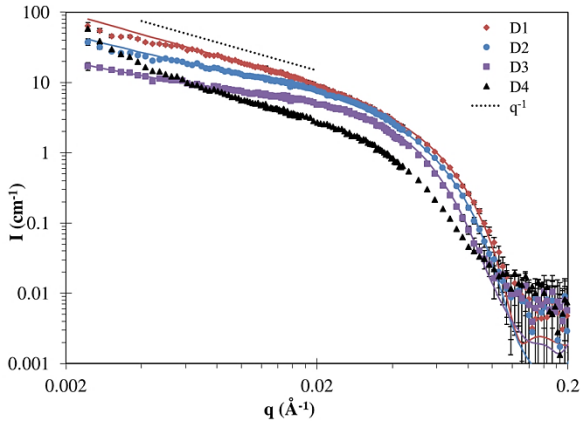

Figure 2. SANS intensity (I (cm^{-1})) versus scattering vector (q) for PDMAc-U_2 (**D1**, **D2**, **D3** and **D4**) solution in D_2O at 10 g L^{-1} and 20 °C. The plain curves are fits according to a model for core-shell cylinder with a circular cross-section (characteristic dimensions in Table 2)

Table 2. Dimensions of the cylindrical micelles, deduced from the fit of SANS data

PDMAc-U_2	Core radius (nm)	Shell thickness (nm)	Volume fraction of short cylinders (ϕ)[a)]	Length of short cylinders (nm)	d_n (cryoTEM) (nm)[b)]
D1	2.6	1.7	0	-	6±1
D2	2.6	2.0	0.55	12	8±1
D3	2.6	2.5	0.85	7	10±2

[a)] The volume fraction of long cylinders is 1-ϕ; [b)] d_n = number-average diameter determined by cryoTEM (cf. Table 1)

Analysis of PDMAc$_{20}$-U_2 (**D2**) and PDMAc$_{35}$-U_2 (**D3**) solutions in deuterated water clearly showed that the increase in molar mass results in a decrease of the scattered intensity that is most significant at low q (below 0.02 Å^{-1}) and also at high q (above 0.04 Å^{-1}). The latter effect is unambiguously due to an increase of the radius of the cross-section, and the former effect is most likely due to a decrease in the length of the cylinders. Fitting of the data with the form factor of a core-shell cylinder with a circular cross-section and a finite length does not yield a satisfactory fit, even with a large dispersity in the length. Since the microscopy experiments showed the presence of both long fibers and much shorter objects, we attempted to fit the data by a combination of long and short cylinders (see for example details of the fitting method for **D3** in Figure S12). The radius of the core was kept constant for the long and short cylinders of both polymers and identical to the one of PDMAc$_{11}$-TTC-U_2 (**D1**) (2.6 nm), since the three polymers share the same hydrophobic core. Figure 2 shows that a good fit is obtained by adjusting only three parameters for each polymer: the proportion of the (infinitely) long cylinders, the shell thickness (identical for both long and short cylinders) and the length of the short cylinders. The results of the calculation indicate (i) an increase in the proportion of short cylinders, (ii) a decrease in their length and (iii) an increase in the shell thickness, when the hydrophilic block length is increased (Table 2). All these trends are in agreement with the anticipated effect of increasing the steric repulsion.[12] For the PDMAc-U_2 with the highest DP_n (**D4**), the scattering features are qualitatively consistent with the previous tendency, but a low

q upturn indicates the presence of aggregates with a larger cross-section. Therefore, a quantitative fit was not attempted. In conclusion, the combined results of cryo-TEM and SANS show that the introduction of a bisurea sticker allows forcing the self-assembly of PDMAc by direct dissolution in water toward cylindrical micelles, but that the proportion of longer cylindrical micelles decreases with increasing length of the PDMAc segment.

To investigate the dynamics and driving forces of the assemblies, isothermal titration calorimetry (ITC) dilution studies at room temperature were performed. Therefore, aliquots of a solution of PDMAc-U_2 at 0.88 mM were injected into pure water present in the calorimetric cell, and the heat flow induced by the partial dissociation of the assemblies was measured at each injection. The results for **D1bis** displayed in Figure 3 show that the disassembly of **D1bis** in water leads to a positive signal (Figure 3A) corresponding to an endothermic process. Consequently, the assembly of **D1bis** in water is exothermic ($\Delta H_{ass.} < 0$), i.e. enthalpy driven, which shows that H-bonding is involved in the association process.[10] Moreover, the ITC dilution experiment proves that the self-assembly of **D1bis** is dynamic. Indeed, after each injection the signal (Figure 3A) reaches the baseline within two minutes, showing the fast dissociation of the assemblies in water. We can therefore also suppose that the aggregate formation by direct dissolution of PDMAc-U_2 in water is at or close to equilibrium. By integrating each peak, the corresponding enthalpogram was established and the critical aggregation concentration (CAC) of **D1bis** was determined to be 0.05 mM (Figure 3B). For concentrations below the CAC, a significant heat exchange was observed revealing the disassembly of the cylindrical micelles. Above this concentration, the measured heat exchange was negligible revealing that the micelles are stable.

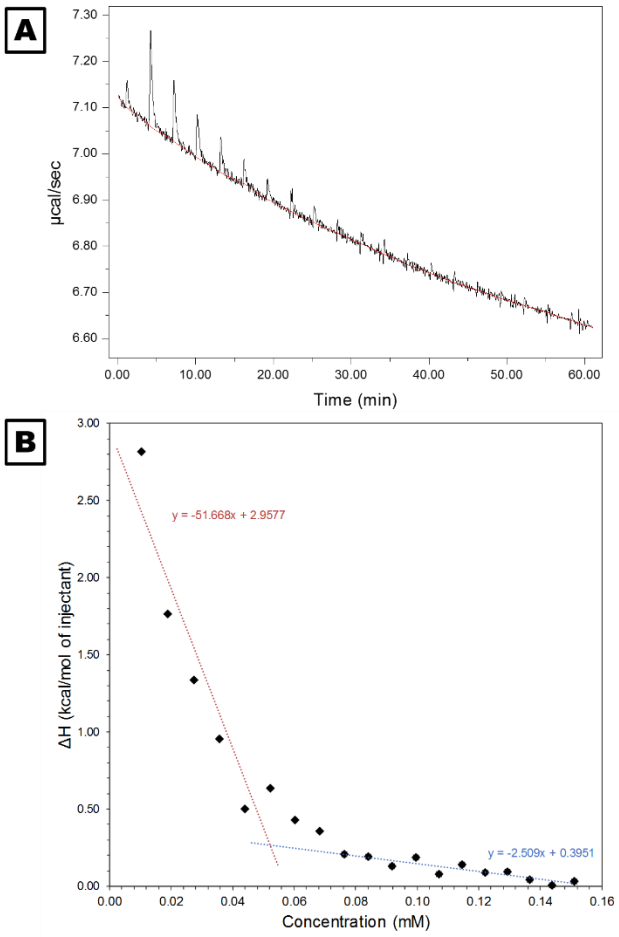

Figure 3. ITC aqueous dilution experiment of a solution of $PDMAc_{11}$-U_2 (**D1bis,** Table S1) at 25°C: (A) Heat effect produced by injecting aliquots of solution of **D1bis** (0.88 mM) in water, (B) the corresponding enthalpogram resulting from the integration of the raw signal and the determination of the CAC for **D1bis**

ITC dilution experiments for longer polymers with DP_n 20 to 40 revealed again an endothermic dissociation mechanism, with similar kinetics. The comparison of the enthalpograms of **D1bis**, **D2bis**, **D3bis** and **D4bis** (Figure S13) indicates that the increase in molar mass results in a decrease of the stability of the assemblies.

Self-assembly of other bisurea-functional polymers in water

In order to test the versatility of our chemical platform, we studied the assembly of the other bisurea-functional polymers, namely poly(acrylic acid) (PAA) **AA2**, polyacrylamide (PAM) **AM2** and poly(2-(*N,N*-dimethylamino)ethyl acrylate) (PDMAEA) **DE3** (Table 1), with comparable DP_n (compare $DP_{n,NMR}$, Table 1), *i.e.* a DP_n for which a majority of cylindrical micelles were obtained with PDMAc. Cryo-TEM analyses of 1 wt% aqueous solutions of PAA_{20}-U_2 (**AA2**) and $PDMAEA_{32}$-U_2 (**DE3**) unambiguously showed the formation of cylindrical micelles, while for PAM_{24}-U_2 (**AM2**) - despite the comparable DP_n - only spherical morphologies were observed (Figure 4A, 4B and 4C). However, decreasing the DP_n of PAM to approximately 10 (PAM_9-U_2, **AM1**), allowed again the formation of cylindrical micelles as shown in Figure 4D. PAM is actually a highly hydrated polymer possessing a high density of sites available for hydrogen bonding. Diluting the structure-directing bisurea moiety in a long PAM seems thus to weaken the supramolecular interactions between the bisurea moieties inhibiting the assembly into long cylindrical structures. In other words, increasing the DP_n disfavors the filamentous morphology as previously observed and discussed for PDMAc. The critical DP_n for which long cylinders become negligible depends on the chemistry of the polymer and is markedly lower for PAM compared to PDMAc, for which a majority of long cylindrical micelles was observed at $DP_n = 20$ (and are still present - albeit in minority - at $DP_n = 35$).

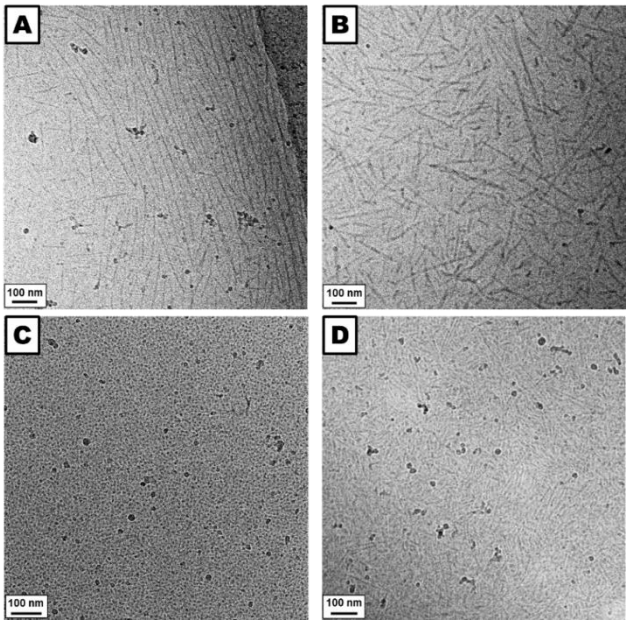

Figure 4. Representative cryo-TEM images of aqueous solutions of (A) PAA_{20}-U_2 **AA2,** (B) $PDMAEA_{32}$-U_2 **DE3**, (C) PAM_{24}-U_2 **AM2**, (D) PAM_{9}-U_2 **AM1** of prepared at 1 wt% by direct dissolution in water (natural $pH(AA2)_{aq}$ = 3.9, $pH(DE3)_{aq}$ = 9.5). The dark spots are contaminations stemming from water crystals on the sample surface.

The results show that the structure directing bisurea-moiety is not only a valuable structure directing unit for assembling PDMAc polymers into cylindrical micelles, but is also compatible with other hydrophilic polymers such as highly H-bond competing PAM or PAA.

pH-responsive assembly and disassembly of cylindrical micelles

In the previous studies, the morphology of the assemblies was studied after spontaneous dissolution of the bisurea-functional polymer in water, without adjusting the pH. Interestingly, the formation of well-defined and long cylindrical micelles was also observed for the bisurea-functional polyelectrolyte PAA-U_2 **AA2** (Figure 5B, Table 1). In this case, the natural pH of the solution was measured to be 3.9. In order to assess the impact of the pH on the PAA-U_2

assembly, the pH was changed after its dissolution in water, either diminished to 2.7 or increased to pH 7.8 (the apparent pK_a value of the PAA (ionization degree of 50%) is 5.8[56]).

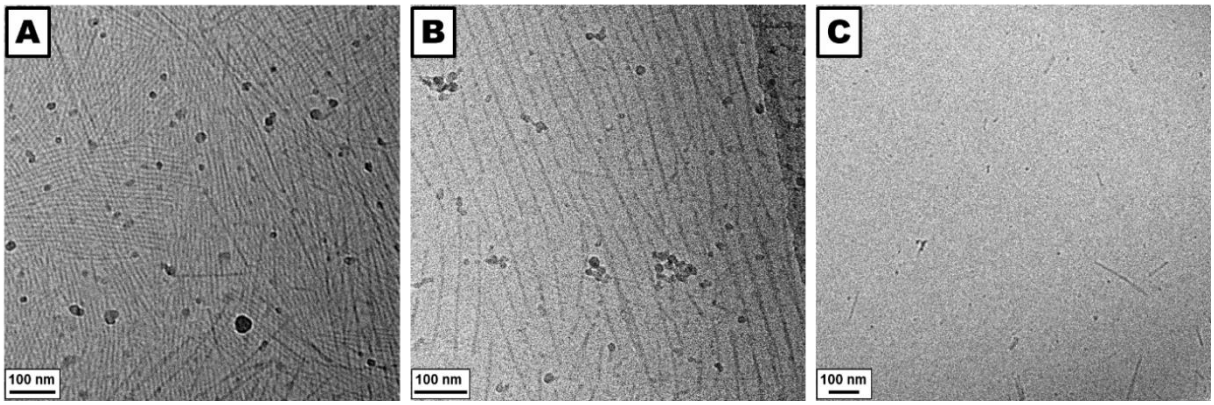

Figure 5. Representative cryo-TEM images of PAA-U_2 (**AA2**) nano-objects prepared at room temperature at 1 wt% in water at different pH: (A) pH = 2.7, (B) pH = 3.9 and (C) pH = 7.8. The dark spots are contaminations stemming from water crystals on the sample surface.

Firstly, the solution was observed with naked eye: it remained clear from 3.9 to 7.8 but turned turbid when decreasing the pH to 2.7, indicating the formation of large aggregates. The cryo-TEM image in Figure 5A showed that decreasing the pH to 2.7, triggered the aggregation of the cylindrical micelles. On the other hand, increasing the pH to 7.8 led to their disassembly: only a few cylindrical micelles and some spherical micelles could be detected by cryo-TEM. Increasing the pH indeed increases the ionization degree of the AA units[57], and the observed disassembly may thus be explained by electrostatic repulsions in the PAA brush that overrule directional supramolecular interaction of the bisurea moieties. On the other hand, decreasing the pH decreases the ionization degree of PAA and interaction between carboxylic acid groups become possible through H-bonding leading to a pH-controlled aggregation of the filaments.

It should be mentioned that Gosh group has recently reported the formation of cylindrical micelles driven by the supramolecular interaction of the naphthalene diimide functionality.[38] They actually studied the pH dependent assembly of a poly(*N*-methacryloyl-4-aminobutanoic

acid) obtained by post-polymerization functionalization of a parent amine-reactive functional polymer. In water (without pH adjustment) spherical micelles spontaneously formed that transformed upon aging – at least partially - into cylindrical micelles. At pH = 10 however bundles of cylinders were observed that did not alter upon aging. This behavior is clearly different from our observations and might be attributed to the difference in chemistry of the supramolecular sticker or the polymer.

Conclusion

In summary, we designed a RAFT agent functionalized by a bisurea sticker (U_2) allowing the straightforward synthesis of polymers possessing a single supramolecular structure-directing unit (SSDU) which drives the spontaneous assembly of the polymers in water towards long cylindrical micelles. By using the RAFT technology, various well-defined polymers are directly accessible in one step - without post-polymerization modification steps, which generally include laborious separation of functional from unfunctional polymer. Cryo-TEM and SANS analyses of a series of bisurea functionalized PDMAc (PDMAc-U_2) solutions revealed the formation of cylindrical micelles, whose length and abundance decreased with increasing M_n of the polymer. For the longest polymers steric effects clearly overrule the directed sticker interactions. Moreover, blank experiments with a bisurea-free octadecyl-capped model PDMAc proved that directional H-bonding (originating from the bisurea sticker) is clearly responsible for the one-dimensional self-assembly into cylindrical micelles. ITC dilution experiment confirmed that the association is dynamic and enthalpy-driven, thus proving the role of H-bonding interactions. It was further shown that the spontaneous supramolecular assembly into cylindrical micelles *via* a bisurea sticker was not restricted to PDMAc but could also be extended to polyacrylamide and other ionic polyacrylates, such as poly(*2-(N,N*-dimethylamino)ethyl acrylate) or poly(acrylic acid). Interestingly with the latter, the

assembly/disassembly of the cylindrical micelle was pH-responsive and thus the aggregation could be controlled by tuning the pH. On the basis of these results, we believe that combining polymer functionalization through RAFT polymerization and directional supramolecular interactions is a strong and versatile strategy to achieve a wide range of filamentous micelles for various applications.

ASSOCIATED CONTENT

Supporting information

The Supporting Information is available free of charge on the ACS Publications website at DOI: 10.1021/acs.macromol.XXX.

Experimental details and additional data. Schemes S1 and S2, Figures S1-S13 and Tables S1 and S2. (PDF)

AUTHOR INFORMATION

Corresponding authors

*E-mail: francois.stoffelbach@sorbonne-universite.fr (F.S.).

*E-mail : jutta.rieger@sorbonne-universite.fr (J.R.).

ORCID

Jutta Rieger: 0000-0001-9391-4917

François Stoffelbach: 0000-0001-6215-2825

Notes

The authors declare no competing financial interest

ACKNOWLEDGMENT

J.R. thanks the Agence Nationale de la Recherche (PISAForFilms project, ANR-17-CE09-0031-01). The authors thank Justine Elgoyhen for technical support.

REFERENCES

(1) Blanazs, A.; Verber, R.; Mykhaylyk, O. O.; Ryan, A. J.; Heath, J. Z.; Douglas, C. W. I.; Armes, S. P. Sterilizable Gels from Thermoresponsive Block Copolymer Worms. *J. Am. Chem. Soc.* **2012**, *134* (23), 9741–9748.

(2) Albigès, R.; Klein, P.; Roi, S.; Stoffelbach, F.; Creton, C.; Bouteiller, L.; Rieger, J. Water-Based Acrylic Coatings Reinforced by PISA-Derived Fibers. *Polym. Chem.* **2017**, *8*, 4992–4995.

(3) Khalily, M. A.; Ustahuseyin, O.; Garifullin, R.; Genc, R.; Guler, M. O. A Supramolecular Peptide Nanofiber Templated Pd Nanocatalyst for Efficient Suzuki Coupling Reactions under Aqueous Conditions. *Chem. Commun.* **2012**, *48* (92), 11358–11360.

(4) Mable, C. J.; Thompson, K. L.; Derry, M. J.; Mykhaylyk, O. O.; Binks, B. P.; Armes, S. P. ABC Triblock Copolymer Worms: Synthesis, Characterization, and Evaluation as Pickering Emulsifiers for Millimeter-Sized Droplets. *Macromolecules* **2016**, *49* (20), 7897–7907.

(5) Krieg, E.; Bastings, M. M. C.; Besenius, P.; Rybtchinski, B. Supramolecular Polymers in Aqueous Media. *Chem. Rev.* **2016**, *116* (4), 2414–2477.

(6) Rehm, T.; Schmuck, C. How to Achieve Self-Assembly in Polar Solvents Based on Specific Interactions? Some General Guidelines. *Chem. Commun.* **2008**, *0* (7), 801–813.

(7) Chebotareva, N.; Bomans, P. H. H.; Frederik, P. M.; Sommerdijk, N. A. J. M.; Sijbesma, R. P. Morphological Control and Molecular Recognition by Bis-Urea Hydrogen Bonding in Micelles of Amphiphilic Tri-Block Copolymers. *Chem. Commun.* **2005**, *0* (39), 4967–4969.

(8) Pal, A.; Karthikeyan, S.; Sijbesma, R. P. Coexisting Hydrophobic Compartments through Self-Sorting in Rod-like Micelles of Bisurea Bolaamphiphiles. *J. Am. Chem. Soc.* **2010**, *132* (23), 7842–7843.

(9) Koenigs, M. M. E.; Pal, A.; Mortazavi, H.; Pawar, G. M.; Storm, C.; Sijbesma, R. P. Tuning Cross-Link Density in a Physical Hydrogel by Supramolecular Self-Sorting. *Macromolecules* **2014**, *47* (8), 2712–2717.

(10) Obert, E.; Bellot, M.; Bouteiller, L.; Andrioletti, F.; Lehen-Ferrenbach, C.; Boué, F. Both Water- and Organo-Soluble Supramolecular Polymer Stabilized by Hydrogen-Bonding and Hydrophobic Interactions. *J. Am. Chem. Soc.* **2007**, *129* (50), 15601–15605.

(11) Fuchise, K.; Kakuchi, R.; Lin, S.-T.; Sakai, R.; Sato, S.-I.; Satoh, T.; Chen, W.-C.; Kakuchi, T.; Control of Thermoresponsive Property of Urea End-functionalized Poly(N-isopropylacrylamide) Based on the Hydrogen Bond-assisted Self-assembly in Water. *J. Polym. Sci. Part A: Polym. Chem.* **2009**, *47* (22), 6259–6268.

(12) Dankers, P. Y. W.; Hermans, T. M.; Baughman, T. W.; Kamikawa, Y.; Kieltyka, R. E.; Bastings, M. M. C.; Janssen, H. M.; Sommerdijk, N. A. J. M.; Larsen, A.; Luyn, M. J. A. van; et al. Hierarchical Formation of Supramolecular Transient Networks in Water: A Modular Injectable Delivery System. *Adv. Mater.* **2012**, *24* (20), 2703–2709.

(13) Larnaudie, S. C.; Brendel, J. C.; Romero-Canelón, I.; Sanchez-Cano, C.; Catrouillet, S.; Sanchis, J.; Coverdale, J. P. C.; Song, J.-I.; Habtemariam, A.; Sadler, P. J.; et al. Cyclic Peptide–Polymer Nanotubes as Efficient and Highly Potent Drug Delivery Systems for Organometallic Anticancer Complexes. *Biomacromolecules* **2018**, *19* (1), 239–247.

(14) Catrouillet, S.; Brendel, J. C.; Larnaudie, S.; Barlow, T.; Jolliffe, K. A.; Perrier, S. Tunable Length of Cyclic Peptide–Polymer Conjugate Self-Assemblies in Water. *ACS Macro Lett.* **2016**, *5* (10), 1119–1123.

(15) Mansfield, E. D. H.; Hartlieb, M.; Catrouillet, S.; Rho, J. Y.; Larnaudie, S. C.; Rogers, S. E.; Sanchis, J.; Brendel, J. C.; Perrier, S. Systematic Study of the Structural Parameters Affecting the Self-Assembly of Cyclic Peptide–Poly(Ethylene Glycol) Conjugates. *Soft Matter* **2018**, *14* (30), 6320–6326.

(16) Yoon, S.; Nichols, W. T. Cyclodextrin Directed Self-Assembly of TiO2 Nanoparticles. *Appl. Surf. Sci.* **2013**, *285*, 517–523.
(17) Leenders, C. M. A.; Albertazzi, L.; Mes, T.; Koenigs, M. M. E.; Palmans, A. R. A.; Meijer, E. W. Supramolecular Polymerization in Water Harnessing Both Hydrophobic Effects and Hydrogen Bond Formation. *Chem. Commun.* **2013**, *49* (19), 1963–1965.
(18) Garzoni, M.; Baker, M. B.; Leenders, C. M. A.; Voets, I. K.; Albertazzi, L.; Palmans, A. R. A.; Meijer, E. W.; Pavan, G. M. Effect of H-Bonding on Order Amplification in the Growth of a Supramolecular Polymer in Water. *J. Am. Chem. Soc.* **2016**, *138* (42), 13985–13995.
(19) Saez Talens, V.; Englebienne, P.; Trinh, T. T.; Noteborn, W. E. M.; Voets, I. K.; Kieltyka, R. E. Aromatic Gain in a Supramolecular Polymer. *Angew. Chem. Int. Ed.***2015**, *54* (36), 10502–10506.
(20) Kim, B.-S.; Hong, D.-J.; Bae, J.; Lee, M. Controlled Self-Assembly of Carbohydrate Conjugate Rod−Coil Amphiphiles for Supramolecular Multivalent Ligands. *J. Am. Chem. Soc.* **2005**, *127* (46), 16333–16337.
(21) Hendrikse, S. I. S.; Wijnands, S. P. W.; Lafleur, R. P. M.; Pouderoijen, M. J.; Janssen, H. M.; Dankers, P. Y. W.; Meijer, E. W. Controlling and Tuning the Dynamic Nature of Supramolecular Polymers in Aqueous Solutions. *Chem. Commun.* **2017**, *53* (14), 2279–2282.
(22) Marakis, J.; Wunderlich, K.; Klapper, M.; Vlassopoulos, D.; Fytas, G.; Müllen, K. Strong Physical Hydrogels from Fibrillar Supramolecular Assemblies of Poly(Ethylene Glycol) Functionalized Hexaphenylbenzenes. *Macromolecules* **2016**, *49* (9), 3516–3525.
(23) Jenkins, A. D.; Jones, R. G.; Moad, G. Terminology for Reversible-Deactivation Radical Polymerization Previously Called "Controlled" Radical or "Living" Radical Polymerization (IUPAC Recommendations 2010). *Pure Appl. Chem.* **2009**, *82* (2).
(24) Save, M.; Guillaneuf, Y.; Gilbert, R. G. Controlled Radical Polymerization in Aqueous Dispersed Media. *Australian Journal of Chemistry* **2006**, *59* (10), 693.
(25) Zetterlund, P. B.; Thickett, S. C.; Perrier, S.; Bourgeat-Lami, E.; Lansalot, M. Controlled/Living Radical Polymerization in Dispersed Systems: An Update. *Chem. Rev.* **2015**, *115* (18), 9745–9800.
(26) Chiefari, J.; Chong, Y. K. (Bill); Ercole, F.; Krstina, J.; Jeffery, J.; Le, T. P. T.; Mayadunne, R. T. A.; Meijs, G. F.; Moad, C. L.; Moad, G.; et al. Living Free-Radical Polymerization by Reversible Addition−Fragmentation Chain Transfer: The RAFT Process. *Macromolecules* **1998**, *31* (16), 5559–5562..
(27) Bernard, J.; Lortie, F.; Fenet, B. Design of Heterocomplementary H-Bonding RAFT Agents - Towards the Generation of Supramolecular Star Polymers. *Macromol. Rapid Commun.* **2009**, *30* (2), 83–88.
(28) Chen, S.; Bertrand, A.; Chang, X.; Alcouffe, P.; Ladavière, C.; Gérard, J.-F.; Lortie, F.; Bernard, J. Heterocomplementary H-Bonding RAFT Agents as Tools for the Preparation of Supramolecular Miktoarm Star Copolymers. *Macromolecules* **2010**, *43* (14), 5981–5988.
(29) Bertrand, A.; Lortie, F.; Bernard, J. Routes to Hydrogen Bonding Chain-End Functionalized Polymers. *Macromol. Rapid Commun.***2012**, *33* (24), 2062–2091.
(30) Chen, S.; Deng, Y.; Chang, X.; Barqawi, H.; Schulz, M.; Binder, W. H. Facile Preparation of Supramolecular (ABAC)n Multiblock Copolymers from Hamilton Wedge and Barbiturate-Functionalized RAFT Agents. *Polym. Chem.* **2014**, *5* (8), 2891–2900.
(31) Celiz, A. D.; Lee, T.-C.; Scherman, O. A. Polymer-Mediated Dispersion of Gold Nanoparticles: Using Supramolecular Moieties on the Periphery. *Advanced Materials* **2009**, *21* (38–39), 3937–3940.
(32) Celiz, A. D.; Scherman, O. A. A Facile Route to Ureidopyrimidinone-Functionalized Polymers via RAFT. *J. Polym. Sci. Part A: Polym. Chem.* **2010**, *48* (24), 5833–5841.

https://doi.org/10.1002/pola.24391.
(33) Xu, J.; Tao, L.; Boyer, C.; Lowe, A. B.; Davis, T. P. Facile Access to Polymeric Vesicular Nanostructures: Remarkable ω-End Group Effects in Cholesterol and Pyrene Functional (Co)Polymers. *Macromolecules* **2011**, *44* (2), 299–312.
(34) Chen, M.; Ghiggino, K. P.; Launikonis, A.; Mau, A. W. H.; Rizzardo, E.; Sasse, W. H. F.; Thang, S. H.; Wilson, G. J. RAFT Synthesis of Linear and Star-Shaped Light Harvesting Polymers Using Di- and Hexafunctional Ruthenium Polypyridine Reagents. *J. Mater. Chem.* **2003**, *13* (11), 2696–2700.
(35) Zhou, G.; Harruna, I. I. Synthesis and Characterization of Tris(2,2'-Bipyridine)Ruthenium(II)-Centered Polystyrenes via Reversible Addition−Fragmentation Chain Transfer (RAFT) Polymerization. *Macromolecules* **2004**, *37* (19), 7132–7139.
(36) Boyer, C.; Bulmus, V.; Liu, J.; Davis, T. P.; Stenzel, M. H.; Barner-Kowollik, C. Well-Defined Protein−Polymer Conjugates via in Situ RAFT Polymerization. *J. Am. Chem. Soc.* **2007**, *129* (22), 7145–7154.
(37) Pramanik, P.; Ray, D.; Aswal, V. K.; Ghosh, S. Supramolecularly Engineered Amphiphilic Macromolecules: Molecular Interaction Overrules Packing Parameters. *Angew. Chem.* **2017**, *129* (13), 3570–3574.
(38) Dey, P.; Rajdev, P.; Pramanik, P.; Ghosh, S. Specific Supramolecular Interaction Regulated Entropically Favorable Assembly of Amphiphilic Macromolecules. *Macromolecules* **2018**.
(39) Holder, S. J.; Sommerdijk, N. A. J. M. New Micellar Morphologies from Amphiphilic Block Copolymers: Disks, Toroids and Bicontinuous Micelles. *Polymer Chemistry* **2011**, *2* (5), 1018. https://doi.org/10.1039/c0py00379d.
(40) Israelachvili, J. N. *Int. Surf. Forces*, 3. ed.; Elsevier, Acad. Press: Amsterdam, 2011.
(41) Blanazs, A.; Armes, S. P.; Ryan, A. J. Self-Assembled Block Copolymer Aggregates: From Micelles to Vesicles and Their Biological Applications. *Macromol. Rapid Commun.* **2009**, *30* (4–5), 267–277.
(42) Melia, K.; Greenland, B. W.; Hermida-Merino, D.; Hart, L. R.; Hamley, I. W.; Colquhoun, H. M.; Slark, A. T.; Hayes, W. Self-Assembling Unsymmetrical Bis-Ureas. *React. Funct. Polym.* **2018**, *124*, 156–161.
(43) Couvreur, L.; Lefay, C.; Belleney, J.; Charleux, B.; Guerret, O.; Magnet, S. First Nitroxide-Mediated Controlled Free-Radical Polymerization of Acrylic Acid. *Macromolecules* **2003**, *36* (22), 8260–8267.
(44) Adrian, M.; Dubochet, J.; Lepault, J.; McDowall, A. W. Cryo-Electron Microscopy of Viruses. *Nature* **1984**, *308* (5954), 32–36.
(45) Lesage de La Haye, J.; Guigner, J.-M.; Marceau, E.; Ruhlmann, L.; Hasenknopf, B.; Lacôte, E.; Rieger, J. Amphiphilic Polyoxometalates for the Controlled Synthesis of Hybrid Polystyrene Particles with Surface Reactivity. *Chem. Eur. J.* **2015**, *21* (7), 2948–2953.
(46) Dubochet, J.; Adrian, M.; Chang, J. J.; Homo, J. C.; Lepault, J.; McDowall, A. W.; Schultz, P. Cryo-Electron Microscopy of Vitrified Specimens. *Q. Rev. Biophys.* **1988**, *21* (2), 129–228.
(47) Arnaud, A.; Bouteiller, L. Isothermal Titration Calorimetry of Supramolecular Polymers. *Langmuir* **2004**, *20* (16), 6858–6863.
(48) SasView http://www.sasview.org/ (accessed Aug 29, 2018).
(49) Stokes, K.; Beyer, F. L. Synthesis and Characterization of Phosphonium-Containing Cationic Poly (Styrene) Polymers. *Polymer Preprints* **2010**, *51*, 709.
(50) Mellot, G.; Beaunier, P.; Guigner, J.-M.; Bouteiller, L.; Rieger, J.; Stoffelbach, F. Beyond Simple AB Diblock Copolymers: Application of Bifunctional and Trifunctional RAFT Agents to PISA in Water. *Macromol. Rapid Commun.* **2019**,

https://doi.org/10.1002/marc.201800315.
(51) Han, G.; Tamaki, M.; Hruby, V. J. Fast, Efficient and Selective Deprotection of the Tert-Butoxycarbonyl (Boc) Group Using HCl/Dioxane (4 M). *Chem. Biol. Drug Design* **2001**, *58* (4), 338–341.
(52) Kautz, H.; van Beek, D. J. M.; Sijbesma, R. P.; Meijer, E. W. Cooperative End-to-End and Lateral Hydrogen-Bonding Motifs in Supramolecular Thermoplastic Elastomers. *Macromolecules* **2006**, *39* (13), 4265–4267.
(53) Sambe, L.; Belal, K.; Stoffelbach, F.; Lyskawa, J.; Delattre, F.; Bria, M.; Sauvage, F. X.; Sliwa, M.; Humblot, V.; Charleux, B.; et al. Multi-Stimuli Responsive Supramolecular Diblock Copolymers. *Polym. Chem.* **2014**, *5* (3), 1031–1036.
(54) Tharcis, M.; Breiner, T.; Belleney, J.; Boué, F.; Bouteiller, L. Hydrogen Bonded Supramolecular Polymers in Protic Solvents: Role of Multitopicity. *Polym. Chem.* **2012**, *3* (11), 3093.
(55) Catrouillet, S.; Fonteneau, C.; Bouteiller, L.; Delorme, N.; Nicol, E.; Nicolai, T.; Pensec, S.; Colombani, O. Competition Between Steric Hindrance and Hydrogen Bonding in the Formation of Supramolecular Bottle Brush Polymers. *Macromolecules* **2013**, *46* (19), 7911–7919.
(56) Mori, H.; Müller, A. H. E.; Klee, J. E. Intelligent Colloidal Hybrids via Reversible PH-Induced Complexation of Polyelectrolyte and Silica Nanoparticles. *J. Am. Chem. Soc.* **2003**, *125* (13), 3712–3713.
(57) Charbonneau, C.; Chassenieux, C.; Colombani, O.; Nicolai, T. Controlling the Dynamics of Self-Assembled Triblock Copolymer Networks via the PH. *Macromolecules* **2011**, *44* (11), 4487–4495.